Check for updates

Received: 5 August 2022 | Revised: 28 November 2022 | Accepted: 29 November 2022

DOI: 10.1111/ejn.15901

RESEARCH REPORT

EJN European Journal of Neuroscience FENS WILEY

Reduced resilience of brain state transitions in anti-*N*-methyl-D-aspartate receptor encephalitis

Nina von Schwanenflug[1,2] | **Juan P. Ramirez-Mahaluf**[3] | **Stephan Krohn**[1,2] | **Amy Romanello**[1,2] | **Josephine Heine**[1] | **Harald Prüss**[1,4] | **Nicolas A. Crossley**[3,5,6,7] | **Carsten Finke**[1,2]

[1]Department of Neurology and Experimental Neurology, Charité - Universitätsmedizin Berlin, Berlin, Germany

[2]Berlin School of Mind and Brain, Humboldt-Universität zu Berlin, Berlin, Germany

[3]Department of Psychiatry, School of Medicine, Pontificia Universidad Católica de Chile, Santiago, Chile

[4]German Centre for Neurodegenerative Diseases (DZNE) Berlin, Berlin, Germany

[5]Biomedical Imaging Center, Pontificia Universidad Católica de Chile, Santiago, Chile

[6]Millennium Nucleus for Cardiovascular Magnetic Resonance, Santiago, Chile

[7]Institute of Psychiatry, Psychology and Neuroscience, King's College London, London, UK

Correspondence
Carsten Finke, Department of Neurology and Experimental Neurology, Charité - Universitätsmedizin Berlin, Freie Universität Berlin, Humboldt-Universität zu Berlin, and Berlin Institute of Health, Charitéplatz 1, Berlin 10117, Germany.
Email: carsten.finke@charite.de

Funding information
Deutsche Forschungsgemeinschaft,

Abstract

Patients with anti-*N*-methyl-aspartate receptor (NMDA) receptor encephalitis suffer from a severe neuropsychiatric syndrome, yet most patients show no abnormalities in routine magnetic resonance imaging. In contrast, advanced neuroimaging studies have consistently identified disrupted functional connectivity in these patients, with recent work suggesting increased volatility of functional state dynamics. Here, we investigate these network dynamics through the spatiotemporal trajectory of meta-state transitions, yielding a time-resolved account of brain state exploration in anti-NMDA receptor encephalitis. To this end, resting-state functional magnetic resonance imaging data were acquired in 73 patients with anti-NMDA receptor encephalitis and 73 age- and sex-matched healthy controls. Time-resolved functional connectivity was clustered into brain meta-states, giving rise to a time-resolved transition network graph with states as nodes and transitions between brain meta-states as weighted, directed edges. Network topology, robustness and transition cost of these transition networks were compared between groups. Transition networks of patients showed significantly lower local efficiency ($t = -2.41$, $p_{FDR} = .029$), lower robustness ($t = -2.01$, $p_{FDR} = .048$) and higher leap size ($t = 2.18$, $p_{FDR} = .037$) compared with controls. Furthermore, the ratio of within-to-between module transitions and state similarity was significantly lower in patients. Importantly, alterations of brain state transitions correlated with disease severity. Together, these findings reveal systematic alterations of transition networks in patients, suggesting that anti-NMDA receptor encephalitis is characterized by reduced stability of brain state transitions and that this

List of abbreviations: BOLD signal, blood-oxygen-level-dependent signal; DAMS, distance across meta-states; dATT, dorsal attention network; DMN, default mode network; FC, functional connectivity; FD, framewise displacement; FDR, false discovery rate; FPN, fronto-parietal network; HC, healthy controls; LIM, limbic network; MRI, magnetic resonance imaging; mRS, modified Rankin Scale; NMDAR, anti-*N*-methyl-aspartate receptor; $ratio_{sim}$, ratio of within-to-between meta-state similarity; $ratio_{trans}$, ratio of within-to-between meta-state trasnitions; ROI, region of interest; rs-fMRI, resting-state fMRI; SC, subcortical network; SM, sensorimotor network; TE, echo time; TR, repitition time; vATT, ventral attention network; VIS, visual network.

This is an open access article under the terms of the Creative Commons Attribution-NonCommercial License, which permits use, distribution and reproduction in any medium, provided the original work is properly cited and is not used for commercial purposes.
© 2022 The Authors. *European Journal of Neuroscience* published by Federation of European Neuroscience Societies and John Wiley & Sons Ltd.

Grant/Award Numbers: 1274/6-1, 327654276, FI 2309/1-1, FI 2309/2-1; Deutsches Ministerium für Bildung und Forschung, Grant/Award Numbers: 01GM1908D, CONNECT-GENERATE; Helmholtz Association, Grant/Award Number: HIL-A03; Agencia Nacional de Investigación y Desarrollo, Grant/Award Numbers: 1200601, 3190311, ACT192064

Edited by: Yoland Smith

reduced resilience of transition networks plays a clinically relevant role in the manifestation of the disease.

KEYWORDS

autoimmune encephalitis, functional brain states, functional connectivity dynamics, graph analysis, transition trajectories

1 | INTRODUCTION

Anti-*N*-methyl-aspartate receptor (NMDAR) encephalitis is an immune-mediated disorder of the central nervous system caused by autoantibodies targeting the NMDA receptor and leading to a dysregulation of the glutamatergic neurotransmitter system (Dalmau et al., 2019). The disease manifests in a complex neuropsychiatric syndrome with prominent psychiatric symptoms (e.g., delusions and psychosis) and seizures, dyskinesia, psychosis, decreased levels of consciousness and cognitive dysfunction (Finke et al., 2012; Graus et al., 2016; Heine et al., 2021). Despite the severe disease course, only 50–70% of patients show abnormalities in standard structural magnetic resonance imaging (MRI) (Graus et al., 2016; Heine et al., 2015), resulting in a clinico-radiological paradox. In contrast, several functional MRI studies have suggested disrupted functional connectivity (FC) in NMDAR encephalitis that is linked to disease severity, disease duration and cognitive symptoms (Finke et al., 2012, 2013; Gibson et al., 2019, 2020; Heine et al., 2021; Peer et al., 2017; von Schwanenflug et al., 2022). In contrast, several functional MRI studies have suggested disrupted FC in NMDAR encephalitis that is linked to disease severity, disease duration and cognitive symptoms (Finke et al., 2012, 2013; Gibson et al., 2019, 2020; Heine et al., 2021; Peer et al., 2017; von Schwanenflug et al., 2022). These functional alterations include large-scale functional networks, such as sensorimotor, frontoparietal, lateral-temporal and visual networks (Peer et al., 2017). In addition, the hippocampus and the medial prefrontal cortex—regions with the highest NMDAR density (Dalmau et al., 2011)—have been associated with deficits in memory performance and executive function, two core cognitive symptoms in NMDAR encephalitis (Finke et al., 2012; Heine et al., 2021).

FC as measured with resting-state functional MRI (rs-fMRI) is estimated from the pairwise correlation of blood-oxygen-level-dependent (BOLD) activity between brain regions without the presence of an explicit task (Biswal et al., 1995). However, traditional 'static' approaches obtain FC as an average across several minutes, therefore missing important information that may be derived from dynamic changes in functional connections (Allen et al., 2014; Calhoun et al., 2014). Hence, the analysis of FC has been recently refined from a time-*invariant* static account to a time-*varying* description. This methodological progress allows to unveil temporal properties of functional brain organization, such as the identification of functional states, that is, transient connectivity patterns, and their transition trajectories. These FC dynamics are thought to reflect brain state exploration that facilitates cognition and behaviour and may vary with disease (Bassett et al., 2011; Deco et al., 2011; Kringelbach & Deco, 2020). Accordingly, a recent case–control study investigating FC dynamics in NMDAR encephalitis showed that patients exhibited altered state preference as well as increased transition frequencies between major connectivity patterns (von Schwanenflug et al., 2022). However, a detailed investigation of the transition trajectory of brain states and its link to clinical symptoms is still missing. Brain state exploration—facilitated by transitions between functional states—is thought to ensure stable information representation while promoting functional integration across distant brain regions and subsystems and, if disturbed, potentially affects information integration and behaviour (Deco et al., 2011; Lord et al., 2019). Hence, identifying mechanisms and disruptions of these transition trajectories may contribute to the understanding of the pathophysiology of NMDAR encephalitis and further neuropsychiatric diseases that are associated with NMDAR dysfunction, for example, schizophrenia.

Graph theoretical approaches are well-suited to study the temporal architecture of state exploration. Ramirez-Mahaluf et al. (2020) recently introduced the concept of transition networks to investigate the trajectory of traversing functional states (from hereon also referred to as meta-states). In this concept, transition networks are represented as graphs with brain states as nodes and transitions between meta-states as directed and weighted edges. Similar to other biological systems (Latora & Marchiori, 2001), transition networks show properties of complex networks (i.e., heavy-tailed degree distribution, high local efficiency and modularity) indicating an

14609568, 2023, 3, Downloaded from https://onlinelibrary.wiley.com/doi/10.1111/ejn.15901 by Charité - Universitaetsmedizin, Wiley Online Library on [24/03/2025]. See the Terms and Conditions (https://onlinelibrary.wiley.com/terms-and-conditions) on Wiley Online Library for rules of use; OA articles are governed by the applicable Creative Commons License

organized, cost-efficient, non-random temporal trajectory of brain states (Ramirez-Mahaluf et al., 2020). Furthermore, transition network characteristics have been related to motor function and cognitive performance in healthy controls indicating behavioural relevance (Ramirez-Mahaluf et al., 2020).

Here, we aimed to specify alterations of the spatio-temporal trajectory of state transitions and its relation to disease severity in NMDAR encephalitis. Therefore, we constructed transition networks for a large sample of patients and age- and sex-matched healthy controls. We hypothesized that the temporal structure of state exploration in NMDAR encephalitis would show altered dynamics (von Schwanenflug et al., 2022) and weakened stability of transition networks compared with a group of healthy controls.

2 | MATERIALS AND METHODS

2.1 | Participants

For this study, 73 patients with NMDAR encephalitis were recruited from the Department of Neurology at Charité - Universitätsmedizin Berlin. All patients fulfilled diagnostic criteria including characteristic clinical presentation and detection of IgG NMDA receptor antibodies in the cerebrospinal fluid (Graus et al., 2016). Patients were in the post-acute phase of their disease with a median of 2.97 years (interquartile range [IQR]: 2.48) after disease onset. Disease severity at the time of scan and peak of disease was assessed with the modified Rankin Scale (mRS). The control group consisted of 73 age- and sex-matched healthy participants without any history of neurological or psychiatric disease. Data from 49 patients and 25 controls were analysed in a recent study by von Schwanenflug et al. (2022) investigating functional dynamics in NMDAR encephalitis. For the current study, patient-control matching was optimized for age and sex through a computational matching algorithm (see Data S1). The two groups were perfectly balanced for sex and did not differ significantly in age as tested with a Wilcoxon rank sum test ($p = .61$). Clinical and demographic characteristics are summarized in (Table 1). The study was approved by the ethics committee of the Charité - Universitätsklinikum Berlin and conducted according to the ethical principles of the WMA Declaration of Helsinki.

2.2 | MRI data acquisition

MRI data were collected at the Berlin Center for Advanced Neuroimaging at Charité – Universitätsmedizin Berlin using a 3T Trim Trio scanner equipped with a 20-channel head coil (Siemens, Erlangen, Germany). RS functional images were acquired using an echoplanar imaging sequence (repetition time [TR] = 2.25 s, echo time [TE] = 30 ms, 260 volumes, voxel size = 3.4 × 3.4 × 3.4 mm^3). High-resolution T1-weighted structural scans were collected using a magnetization-prepared rapid gradient echo sequence (MPRAGE; voxel size = 1 × 1 × 1 mm^3).

TABLE 1 Demographic variables and clinical measures of the participants. Table lists median and interquartile range (IQR) of age, mRS at scan, mRS at peak of disease, disease duration and time between scan and diagnosis. Treatment and medication during disease course were evaluated using a binary scale (present: 'yes' vs. absent: 'no'). Disease duration = days in acute care; *N* = number of participants; mRS = modified Rankin Scale

		NMDAR encephalitis patients	Healthy controls
N		73	73
Sex	Female/male	62/11	62/11
Age (years)	Median ± IQR (*N*)	28.55 ± 8.7 (73)	28.50 ± 8.5 (73)
mRS at scan	Median ± IQR (*N*)	1.00 ± 1.5 (70)	..
mRS at peak of disease	Median ± IQR (*N*)	4 ± 2 (67)	..
Disease duration (hospitalization time)	Median ± IQR (*N*)	67.50 ± 72.00 (68)	..
Years between disease onset and study	Mean ± SD (*N*)	2.97 ± 2.48 (71)	..
First-line treatment		72/73	..
Second-line treatment		37/73	..
Anticonvulsant medication		51/73	..
Antipsychotic medication		48/73	..

Abbreviation: NMDAR, anti-*N*-methyl-aspartate receptor.

14609568, 2023, 3, Downloaded from https://onlinelibrary.wiley.com/doi/10.1111/ejn.15901 by Charité - Universitaetsmedizin, Wiley Online Library on [24/03/2025]. See the Terms and Conditions (https://onlinelibrary.wiley.com/terms-and-conditions) on Wiley Online Library for rules of use; OA articles are governed by the applicable Creative Commons License

2.3 | MRI data analysis

Prior to preprocessing, framewise displacement (FD) was calculated for each participant and assessed against a mean FD cutoff of .50 mm (Eijlers et al., 2019; Power et al., 2014). No participant had a mean FD greater than or equal to .50 mm. For preprocessing, we applied the 'ICA-AROMA+2Phys'-Pipeline proposed by Parkes et al. (2018) to our data: The pipeline included removal of the first 4 volumes of each participant's rs-fMRI scan, volume realignment, slice-timing correction, detrending of BOLD time series, intensity normalization, spatial smoothing with 6 mm full width at half maximum, ICA-AROMA for head motion correction to robustly remove motion-induced signal artefacts from the functional MRI data (Pruim et al., 2015), regression of white matter and cerebrospinal fluid time series to control for physiological fluctuations of non-neuronal origin, demeaning and band-pass filtering to retain frequencies between .008 and .08 Hz.

2.4 | Participant-wise meta-state estimation and transition network construction

The following steps were performed with the same parameters as previously described and evaluated in Ramirez-Mahaluf et al. (2020). Time-series extraction was done using a whole-brain parcellation template with 638 similarly sized regions of interests (ROIs) (Crossley et al., 2013). Extracted functional time series were segmented into 127 consecutive time windows of 2TRs ($\triangleq$4.5 s), which yielded reliable results in previous work (Ramirez-Mahaluf et al., 2020). The comparatively short window length was necessary to be able to meaningfully track state transitions across a large number of meta-states. For each window, FC was estimated between any two ROIs using Multiplication of Temporal Derivatives, a method that is suitable to estimate FC across a range of correlation strengths and (short) window lengths (Shine et al., 2015). The resulting ROI-by-ROI (638-by-638) matrices were then Pearson-correlated, resulting in a 127-by-127 similarity matrix of windows. To obtain discrete brain meta-states, MATLAB-inbuilt k-means clustering was applied to the similarity matrix using 10,000 maximum iterations and 2000 replicates with random initial positions. For each meta-state, all windows belonging to that state were averaged, yielding a mean ROI-by-ROI (638-by-638) connectivity matrix. To scrutinize our analyses across multiple numbers of meta-states, we extracted k meta-states ($k = 35$, 40, 45, 50 and 55) following the range of k in (Ramirez-Mahaluf et al., 2020) for each participant separately.

Finally, transition networks were constructed for each participant and k number of meta-states: A transition network is a graph network, where each meta-state corresponds to a node and transitions between meta-states represent the edges of that graph. The edges are directed and weighted according to the number of transitions from meta-state i to meta-state j (Ramirez-Mahaluf et al., 2020).

Importantly, this novel approach runs k-means clustering on each individual time series to describe individual temporal trajectories of meta-state transitions. Hence, this approach differs fundamentally from the definition of dynamic FC states across individuals (von Schwanenflug et al., 2022), which searches for common patterns of recurring connectivity on a group level.

2.5 | Group comparisons of transition network properties

From each of the transition networks, we derived three widely used graph theoretical measures (*modularity*, *local efficiency* and *global efficiency*), two custom measures that are thought to capture the biological costs of meta-state transitions (*leap size* and *immobility*) (Ramirez-Mahaluf et al., 2020), as well as one measure that assesses the *robustness* of the network against perturbations. Note that modularity, local and global efficiency and immobility were calculated on the transition matrix (matrix containing the number of transitions between each pair of meta-states) for each participant, whereas leap size was based on the distance matrix (i.e., 1-correlation for each meta-state pair). To assess robustness, we employed the *NetSwan* package available for *R* to randomly remove one node after another from the network and recalculate the size of the largest connected component (Achard, 2006; Lynall et al., 2010). A more detailed description of the graph theoretical metrics is provided in (Table S1).

In addition, *transition frequency*, *ratio of within-to-between module meta-state similarity* and *ratio of within-to-between module transitions* were compared between patients and controls. Here, a 'module' refers to a group of meta-states assigned to the same community as defined by the modularity algorithm (*community_louvain.m*). Whereas transition frequency is calculated as the absolute number of transitions between different meta-states, the ratio of within-to-between meta-state similarity ($ratio_{sim}$) is defined as the average correlation of meta-states within a module

14609568, 2023, 3, Downloaded from https://onlinelibrary.wiley.com/doi/10.1111/ejn.15901 by Charité - Universitaetsmedizin, Wiley Online Library on [24/03/2025]. See the Terms and Conditions (https://onlinelibrary.wiley.com/terms-and-conditions) on Wiley Online Library for rules of use; OA articles are governed by the applicable Creative Commons License

divided by the average correlation of meta-states between modules. Similarly, the ratio of within-to-between module transitions ($ratio_{trans}$) is the absolute number of transitions within the same module divided by the absolute number of transitions between modules.

Between-group comparisons of graph theoretical measures, transition frequencies, $ratio_{sim}$, and $ratio_{trans}$ were assessed by comparing the area under the curve (AUC; MATLAB's *trapz*) between patients and controls. The AUC was calculated from $k = 35$ to $k = 55$ for each metric and participant, which allowed us to derive one inference measure across all number of meta-states. For each metric separately, the AUC was entered into a regression model controlling for head motion (FD), age, and sex as nuisance variables. Group comparisons were performed on the residuals using a permutation-based t-test and FDR-corrected using Benjamini-Hochberg (Benjamini & Hochberg, 1995).

2.6 | Correlation of network properties with disease severity

Next, we investigated the relationship of transition network properties with disease severity of patients. To this end, mRS scores at the time of scanning and disease duration (days in acute care) were *z*-transformed across patients and subsequently averaged, resulting in a composite *z* score for each patient that reflects disease severity clinical disability. The Pearson's correlation coefficient between dynamic network properties and disease severity was obtained and corrected for multiple comparisons.

2.7 | Functional network topology of meta-states

Lastly, each meta-state can be represented by a whole-brain FC matrix (638-by-638), in which each edge corresponds to the coupling strength between two given brain regions. Consequently, we sought to evaluate the spatial differences in functional topology of these edges across all meta-states. To this end, we quantified how much each edge differed across meta-states by computing the distance across meta-states (DAMS), a previously defined summary measure by Krohn and colleagues (Krohn et al., 2021), which is defined as the cumulative difference across a specified state space. Here, this distance was computed for each edge across all possible meta-state comparisons given a particular value of k, then normalized over k, and finally averaged over the applied range of k values. In consequence, we obtain a single distance measure for each edge and participant, where a high value of DAMS between any two ROIs indicates that the connectivity between these regions differs strongly between meta-states. In contrast, a low DAMS indicates that the connectivity between these regions is similar across all meta-states of a transition network. Subsequently, group differences for each edge in the distance matrix were assessed with a two-sample *t* test and FDR-corrected for multiple comparisons using Benjamini–Hochberg (Benjamini & Hochberg, 1995). Finally, the participant-specific DAMS values were averaged across participants to obtain the distance matrix shown in (Figure 4).

3 | RESULTS

3.1 | Group differences in network properties

Group comparisons of graph theoretical measures yielded significantly lower local efficiency ($t = -2.41$, $p_{FDR} = .029$, $d = .40$), higher leap size ($t = 2.18$, $p_{FDR} = .037$, $d = .36$) and lower robustness ($t = -2.01$, $p_{FDR} = .048$, $d = .33$) of transition networks in patients compared with controls. In contrast, modularity ($t = -1.43$, $p_{FDR} = .12$, $d = .27$), global efficiency ($t = 1.00$, $p_{FDR} = .20$, $d = .17$) and immobility ($t = -.32$, $p_{FDR} = .38$, $d = .05$) of transitions networks did not differ between groups (Figure 1). The transition networks of six exemplary participants with high and low leap size are shown in Figure S1.

Correlation of similarity and the number of transitions between two meta-states revealed that transition frequency was higher between similar meta-states for both groups and all numbers of meta-states (rho = [.48, .53, .54, .54, .52] for the different k meta-states; all $p < .001$, Figure 2). Accordingly, transitions within modules were on average 3.4 times more likely than between modules with a $ratio_{trans}$ (ratio of within-to-between module transitions) = [2.40, 2.94, 3.44, 3.89, 4.44] depending on the number of meta-states. This result was expected as modularity is calculated on the transition matrix. Interestingly, however, the $ratio_{trans}$ was significantly lower in patients with NMDAR encephalitis compared to controls ($t = -2.48$, $p_{FDR} = .026$, $d = .40$), whereas the overall number of transitions between different meta-states did not differ between groups ($t = .32$, $p_{FDR} = .377$, $d = .05$). Similar to $ratio_{trans}$, $ratio_{sim}$ (ratio of within-to-between meta-state similarity) was on average 3.2 ($ratio_{sim} = [2.9, 3.1, 3.2, 3.3, 3.4]$, for *the different* k meta-states). Again, the $ratio_{sim}$ was significantly lower in patients compared with controls ($t = -2.48$,

14609568, 2023, 3, Downloaded from https://onlinelibrary.wiley.com/doi/10.1111/ejn.15901 by Charité - Universitaetsmedizin, Wiley Online Library on [24/03/2025]. See the Terms and Conditions (https://onlinelibrary.wiley.com/terms-and-conditions) on Wiley Online Library for rules of use; OA articles are governed by the applicable Creative Commons License

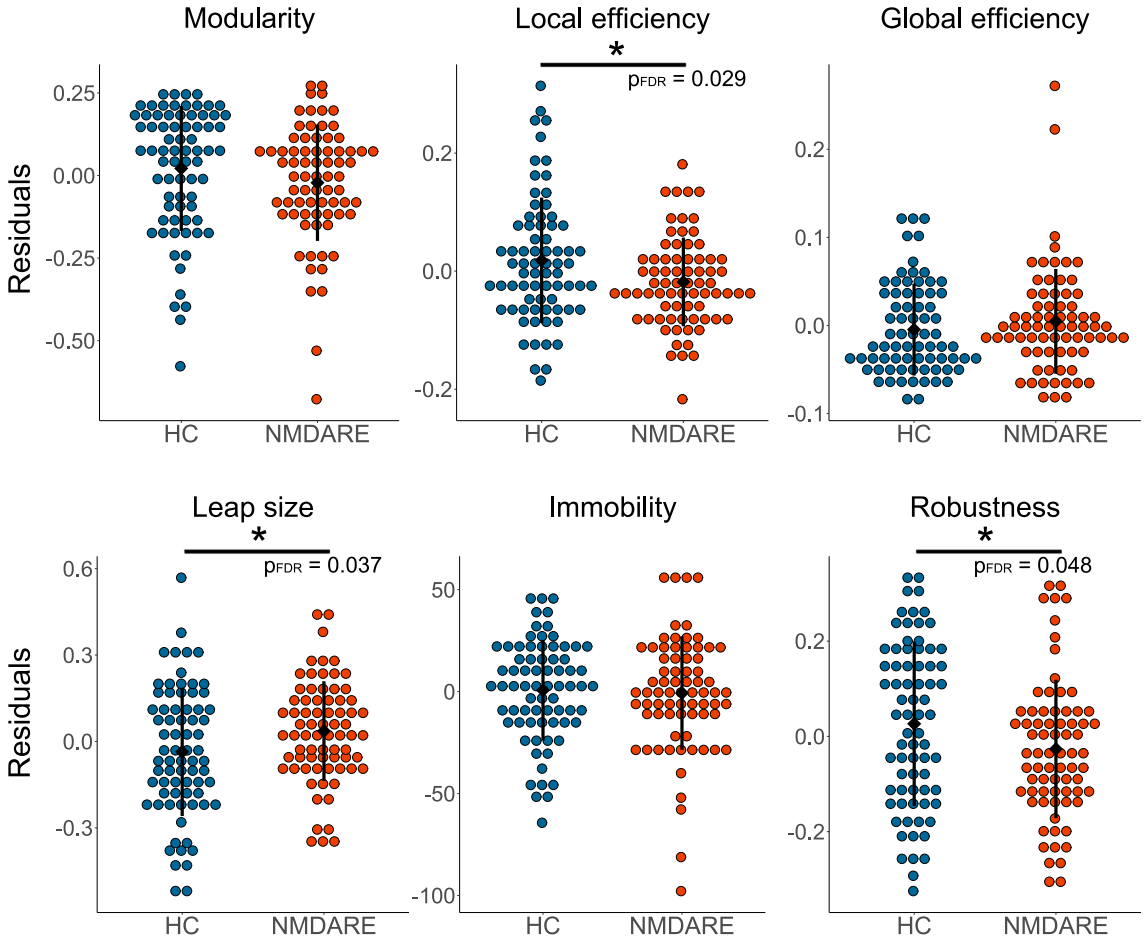

FIGURE 1 Between-group comparisons of graph theoretical measures. Coloured dots represent the residuals after nuisance regression. Black dots and whiskers represent the mean and standard deviation, respectively. HC = healthy controls, NMDAR encephalitis = patients with anti-NMDA receptor encephalitis. * indicates significant difference $p_{FDR} < .05$.

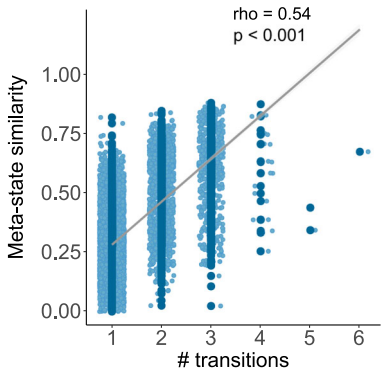

FIGURE 2 Correlation between meta-state similarity and number of transitions between them (here shown for $k = 45$; see Figure S2 for k's = [35, 40, 50, 55]). Meta-state similarity (y-axis) was estimated calculating Spearman's ϱ. The regression line is included for visualization purposes. Number of transitions (x-axis) are the sum of transitions between any two meta-states, independent of the direction of transitions.

$p_{FDR} = .026$, $d = .41$). This suggests that patients transition between topologically more different meta-states (from different modules) compared with controls, whereas the overall transition frequency remains unaltered.

3.2 | Correlation of network properties with disease severity

Next, we investigated the relationship of significant graph metrics, that is, local efficiency, leap size and robustness, ratio_{trans} and ratio_{sim}, with a composite z score for disease severity. Higher disease severity was significantly associated with higher leap size (Pearson's $r = .37$, $p_{FDR} = .0030$, Figure 3), decreased robustness (Pearson's $r = -.37$, $p_{FDR} = .0030$, Figure 3), lower ratio_{sim} (Pearson's $r = -.40$, $p_{FDR} = .0030$, Figure S3) and lower

14609568, 2023, 3, Downloaded from https://onlinelibrary.wiley.com/doi/10.1111/ejn.15901 by Charité - Universitaetsmedizin, Wiley Online Library on [24/03/2025]. See the Terms and Conditions (https://onlinelibrary.wiley.com/terms-and-conditions) on Wiley Online Library for rules of use; OA articles are governed by the applicable Creative Commons License

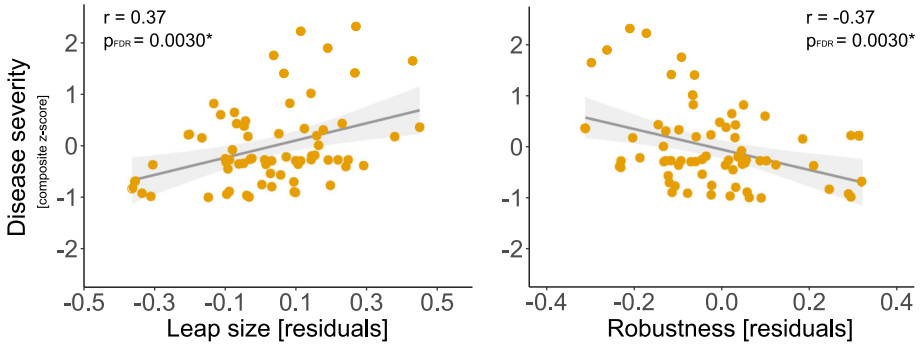

FIGURE 3 Correlation between disease severity (composite z-score) and altered network properties (residuals after nuisance regression). Correlation plots for local efficiency, $ratio_{sim}$ and $ratio_{trans}$ are shown in Figure S3. * indicates significant difference $p_{FDR} < .05$.

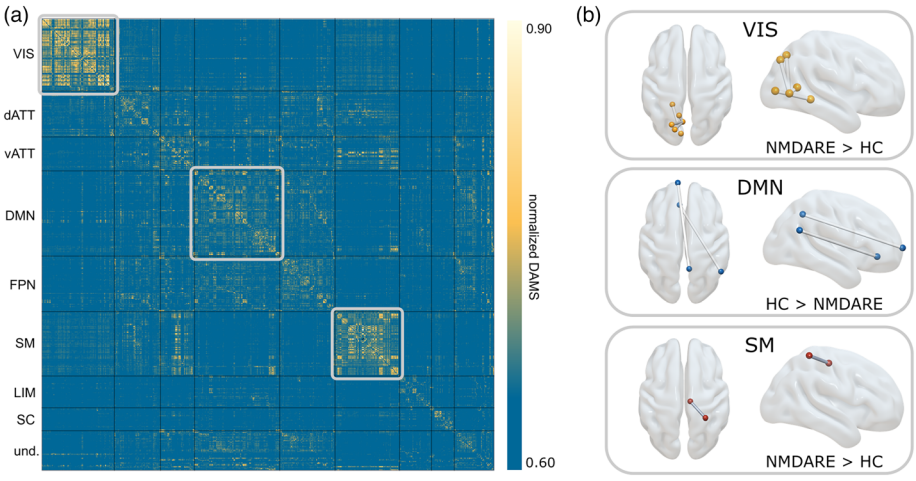

FIGURE 4 Interregional distance across meta-states (DAMS). (a) The DAMS matrix visualizes interregional differences in coupling strength across meta-states averaged across all participants. High DAMS values (yellow) indicate strong differences in connectivity strength across meta-states, whereas low DAMS values (blue) indicate that the connectivity strength between regions is more similar across meta-states. (b) Brain plots show results from group-comparison within each functional network. Differences in DAMS between patients and healthy controls were found for edges within the visual, default-mode and sensorimotor network (false discovery rate [FDR]-corrected). Network assignment of regions is based on the labels proposed by Yeo et al. (2011). Subcortical regions were subsumed as a subcortical network. VIS = visual network, dATT = dorsal attention network, vATT = ventral attention network, DMN = default mode network, FPN = fronto-parietal network, SM = sensorimotor network, LIM = limbic network, SC = subcortical network, und. = undefined, HC = healthy controls, NMDAR encephalitis = patients with anti-NMDA receptor encephalitis.

$ratio_{trans}$ (Pearson's $r = -.33$, $p_{FDR} = .0064$, Figure S3) but not with local efficiency (Pearson's $r = -.11$, $p_{FDR} = .35$, Figure S3).

3.3 | Functional network topology of meta-states

The edges with the highest DAMS, that is, edges that exhibited most pronounced differences in coupling strength across meta-states, clustered predominantly in unimodal networks, namely, the sensorimotor and visual network (Figure 4a). This topological pattern is highly convergent with recent findings from Krohn and colleagues (Krohn et al., 2021) and is akin across groups (Figure S4).

Whole-brain group comparison yielded no significant difference in DAMS between groups after correction for multiple comparison. Therefore, we explored group differences in DAMS within each functional RS network separately. This network-wise group comparison revealed significant differences between edges within the visual, default mode and sensorimotor networks (FDR-corrected, Figure 4b). Remarkably, significant edges showed higher DAMS in patients within the visual and sensorimotor network but lower DAMS within the default-mode network (Table S3).

4 | DISCUSSION

Ongoing brain activity can be described as transient FC patterns (so-called brain states) that are visited in a structured, non-random trajectory (Ramirez-Mahaluf et al., 2020). These brain state dynamics are thought to

14609568, 2023, 3, Downloaded from https://onlinelibrary.wiley.com/doi/10.1111/ejn.15901 by Charité - Universitaetsmedizin, Wiley Online Library on [24/03/2025]. See the Terms and Conditions (https://onlinelibrary.wiley.com/terms-and-conditions) on Wiley Online Library for rules of use; OA articles are governed by the applicable Creative Commons License

facilitate cognition and behaviour and may vary in disease (Kringelbach & Deco, 2020). In this study, we employed a time-resolved analysis of brain activity to capture the spatiotemporal dynamics of brain state transitions in a large sample of patients with NMDAR encephalitis. Our results indicate reduced resilience of state transition networks in patients compared with controls. This manifests in lower local efficiency of the network (fewer transitions from or to neighbouring, i.e., similar and meta-states), higher leap size (transitions between more distinct meta-states) and reduced robustness of the patients' transition networks against random attacks. Furthermore, the ratio of within-to-between module transitions and meta-state similarity was significantly reduced in patients. Importantly, these state dynamic metrics were correlated with disease severity, highlighting the clinical relevance of our findings.

In patients with NMDAR encephalitis, autoantibodies target the NR1 subunit of the NMDA receptor causing an internalization of the receptor (Dalmau et al., 2011). Although this results in a broad range of psychiatric and neurological symptoms, standard clinical MRI shows no or only minor abnormalities in most patients (Graus et al., 2016; Heine et al., 2015). In contrast, FC analyses were able to identify characteristic connectivity alterations: *Static* RS FC analyses that average connectivity across an entire scanning session showed widespread disrupted connectivity in visual, temporal, hippocampal and mid-frontal areas associated with the severity of cognitive and psychiatric symptoms (Cai et al., 2020; Finke et al., 2013; Peer et al., 2017). However, given that brain activity is inherently dynamic (Chang & Glover, 2010), models that incorporate spatiotemporal features of connectivity may complement our knowledge about functional disruptions in neuropsychiatric disorders. Indeed, we recently found that *dynamic* FC showed a shift in state preference and transition probabilities in patients with NMDAR encephalitis that was associated with disease severity and disease duration (von Schwanenflug et al., 2022). In the present study, we further expand on these dynamic FC findings and investigated alterations in the *spatiotemporal trajectory* of functional state exploration through the underlying state space. State exploration is thought to reflect the dynamic repertoire of intrinsic brain activity that is important for information integration and mental processes (Deco et al., 2011; Gu et al., 2017; Lord et al., 2019). Therefore, disruptions in the temporal organization of state transitions may account for clinical symptoms in disease (Deco et al., 2017; Kringelbach & Deco, 2020). In fact, we found a characteristic spatiotemporal reorganization of the transition trajectory in patients compared with controls that was related to disease severity. This spatiotemporal reorganization—as reflected by lower local efficiency, lower robustness and higher leap size of the transition network—may represent overly unstable transition dynamics in NMDAR encephalitis (von Schwanenflug et al., 2022) that could be linked to deficiencies in information integration (Deco et al., 2017; Lord et al., 2019).

At a scale of seconds to minutes, the human brain operates through continuously evolving activity that can be characterized as transient quasi-stable brain states (Allen et al., 2014; Calhoun et al., 2014). This evolution of brain activity is non-random, allowing for a systematic exploration of brain states (Ramirez-Mahaluf et al., 2020). Analogous to the modular spatial organization of the cortex, the temporal trajectory of brain state transitions shows similar topological properties; that is, brain states are grouped into modules of similar meta-states, with higher transition frequencies within a module than between modules (see methods and results section: $ratio_{trans}/ratio_{sim}$). This modular organization is thought to promote segmented and cost-efficient information processing, while enabling the exploration of the functional repertoire via transitions to meta-states of a different module (Bassett et al., 2011; Bertolero et al., 2015; Deco et al., 2017; Sporns & Betzel, 2016; Tognoli & Kelso, 2014). In line with the modular structure, transition networks in healthy controls show high local efficiency and low global efficiency (as compared with a null model) (Ramirez-Mahaluf et al., 2020). Although a high local efficiency allows for locally specialized functioning, a comparatively smaller number of connections between subsystems of a network, that is, low global efficiency, still allow for distributed information processing across different subsystems (Sporns & Betzel, 2016). Moreover, a high local efficiency enhances the robustness of a system. By providing alternative pathways between two nodes (i.e., meta-states), the system compensates for potential disturbances and provides stable representation of information (De Vico Fallani et al., 2009). Interestingly, the spatiotemporal organization of state exploration may also be directly relevant to behaviour. A recent study on transition networks in a healthy population suggests that the efficiency of the network is associated with performance in cognition and motor function (Ramirez-Mahaluf et al., 2020). Thus, state exploration may vary across diseases potentially accounting for a multitude of symptoms (Kringelbach & Deco, 2020).

Indeed, the present study highlights significant differences in the temporal architecture of transition networks between patients with NMDAR encephalitis and healthy controls. We found that patients exhibited decreases in local efficiency and robustness and increases in leap size. Decreased local efficiency hints at unstable

14609568, 2023, 3, Downloaded from https://onlinelibrary.wiley.com/doi/10.1111/ejn.15901 by Charité - Universitaetsmedizin, Wiley Online Library on [24/03/2025]. See the Terms and Conditions (https://onlinelibrary.wiley.com/terms-and-conditions) on Wiley Online Library for rules of use; OA articles are governed by the applicable Creative Commons License

representation of information due to lower redundancy of the transition network, which is described in more detail in the previous paragraph. Leap size is thought to reflect metabolic cost and is measured as the magnitude of 'jumps' between topologically different meta-states. Eliciting state transitions is energetically costly (Gu et al., 2017; Lord et al., 2013) and possibly increases when traversing states that show highly disparate activation profiles. This intuition is supported by our finding that (low-cost) transitions between two similar meta-states are more likely than (cost-intensive) transitions between distant meta-states. Accordingly, higher leap size in patients may indicate higher metabolic demand along with higher volatility of state transitions. Lastly, we evaluated the robustness of the transition network, which is the ability of maintaining information processing within the network before collapsing (Aerts et al., 2016). We found that transition networks of patients with NMDAR encephalitis are less robust compared to those of controls when removing the nodes (i.e., meta-states) one by one. Together with a decreased local efficiency and higher leap size, this points to a destabilization and reduced resilience of transition networks in patients with NMDAR encephalitis, corroborating earlier findings in this patient population (von Schwanenflug et al., 2022). This notion is furthermore supported by decreased ratios of within-to-between module transitions and within-to-between module meta-state similarity in patients. In addition, four out of five network measures—leap size, robustness, $ratio_{trans}$ and $ratio_{sim}$—were correlated with a composite score of disease severity, supporting clinical relevance of our findings.

The neural basis for functional brain state transitions is a matter of ongoing investigation. Neural dynamics may coordinate whole-brain FC patterns, thereby enabling the exploration of the brain's functional repertoire (Gu et al., 2017; Kringelbach & Deco, 2020; Lord et al., 2019). In NMDAR encephalitis, internalization of the NMDAR alters glutamatergic synaptic transmission, impacting the coordination between large-scale functional networks. Interestingly, reduced resilience of transition networks in patients with NMDAR encephalitis is supported by findings from attractor-based computational models that postulate that NMDAR dysfunction may lead to overly unstable attractors in brain activity (Rolls, 2012, 2021). NMDAR hypofunction, as in NMDAR encephalitis and schizophrenia, may lead to a flattening of the attractors (destabilizing effect), facilitating perturbations to provoke transitions between attractors (Loh et al., 2007; Rolls, 2012).

Finally, our study provides evidence that a subset of regions preferentially promotes brain state transitions (Kringelbach & Deco, 2020; Krohn et al., 2021). Convergent with recent work on brain dynamics, we found that changes in connectivity across states are most pronounced in regions of the visual and sensorimotor areas, potentially following a hierarchy from unimodal to transmodal networks (Krohn et al., 2021). Interestingly, in patients with NMDAR encephalitis, connectivity changes across meta-states within unimodal networks were even more pronounced, providing a spatial correlate of the increased temporal volatility in state transitions. Both the visual and the sensorimotor network have been reported to show reduced static FC in patients with NMDAR encephalitis; these effects correlated with disease severity; that is, they were more pronounced in more severely affected patients (Peer et al., 2017). Along with altered FC found in other large-scale functional networks (Chen et al., 2022; Finke et al., 2013; Heine et al., 2015; Peer et al., 2017), these findings reflect the prominent expression of NMDARs throughout the cortex, their pathophysiological role in NMDAR encephalitis and potentially their contribution to the orchestration of brain dynamics. Limiting state transitions to a defined number of regions initiating those transitions raise the intriguing possibility that controlled external stimulation of these particular regions could be applied to achieve a rebalancing of state dynamics (Gu et al., 2017; Kringelbach & Deco, 2020).

Some limitations of our study deserve mentioning: First, statistical comparison of dynamic metrics revealed several significant group differences, albeit with moderate effect sizes. Thus, future work should consider acquiring larger samples and potentially examine subgroup differences in this disease to better characterize the potential clinical significance of these alterations, with the ultimate goal of moving beyond group-level effects and towards individual patients. Second, the window length of 2 TR ($\triangleq$4.5 s) is comparatively short and may decrease the signal-to-noise ratio. However, the size of this time window has been recognized as a good trade-off between sensitivity and specificity (Shine et al., 2015). Furthermore, a high reliability of meta-state estimation was previously shown using a very similar window length (Ramirez-Mahaluf et al., 2020). Third, k-means clustering is applied to each participant separately. Although this approach poses inherent limitations to study between-group differences in meta-state topology, it is particularly suited to investigate individualized temporal dynamics and characteristics of the transition trajectory of functional states. Forth, the applied k enforces the extraction of a large number of (potentially similar) meta-states for each participant. While most studies focus on 3–5 distinct major connectivity states defined on a group level, this number of states may not be sufficient to represent the full repertoire of functional configurations

14609568, 2023, 3, Downloaded from https://onlinelibrary.wiley.com/doi/10.1111/ejn.15901 by Charité - Universitaetsmedizin, Wiley Online Library on [24/03/2025]. See the Terms and Conditions (https://onlinelibrary.wiley.com/terms-and-conditions) on Wiley Online Library for rules of use; OA articles are governed by the applicable Creative Commons License

of the human brain. Furthermore, a small number of states limit a detailed investigation of individual transition trajectories between these states, which was the main purpose of the present study.

5 | CONCLUSION

In this study, we employed a time-resolved graph analytical framework to study the spatiotemporal trajectory of brain state transitions in patients with NMDAR encephalitis. Besides decreases in local efficiency, we observed reduced robustness of the patients' transition networks against random attacks compared with those of healthy controls. Together with higher leap size in patients, these findings show reduced resilience of functional state transitions in patients, that is, related to disease severity. Hence, our findings add to the evidence that disturbance of functional brain network dynamics plays a key role in the pathophysiology of NMDAR encephalitis.

ACKNOWLEDGEMENTS

This study was funded by the Deutsche Forschungsgemeinschaft (DFG, German Research Foundation, grant numbers 327654276 [SFB 1315], FI 2309/1-1, FI 2309/2-1 and PR 1274/6-1) and Deutsches Ministerium für Bildung und Forschung (BMBF, German Ministry of Education and Research, grant number 01GM1908D, CONNECT-GENERATE). HP received funding from the Helmholtz Association (HIL-A03). NS is a doctoral scholar at Cusanuswerk – Bischöfliche Studienförderung. AR is a doctoral scholar at the Berlin School of Mind and Brain, Humboldt-Universität zu Berlin. JRM and NAC were funded by the Agencia Nacional de Investigación y Desarrollo from Chile (ANID), through its programmes FONDECYT postdoctorado (Ref: 3190311 to JRM), FONDECYT regular (Ref: 1200601 to NAC) and Anillo ACT192064. The funders had no influence on study design, data collection, data analyses, data interpretation or writing. Open Access funding enabled and organized by Projekt DEAL.

CONFLICT OF INTEREST

NS, JRM, SK, AR, JH, HP and CF have no competing interests. NAC has received personal fees from Janssen (Johnson & Johnson), outside the submitted work.

AUTHOR CONTRIBUTIONS

Nina von Schwanenflug: Conceptualization; data curation; formal analysis; investigation; methodology; project administration; software; visualization; writing-original draft. **Juan P. Ramirez-Mahaluf:** Conceptualization; formal analysis; investigation; methodology; project administration; software; writing-review and editing. **Stephan Krohn:** Data curation; investigation; methodology; software; supervision; writing-original draft; writing-review and editing. **Amy Romanello:** Formal analysis; investigation; writing-review and editing. **Josephine Heine:** Data curation; writing-review and editing. **Harald Pruess:** Data curation; writing-review and editing. **Nicolas Crossley:** Conceptualization; methodology; writing-review and editing. **Carsten Finke:** Conceptualization; formal analysis; funding acquisition; investigation; methodology; project administration; supervision; writing-original draft; writing-review and editing.

PEER REVIEW

The peer review history for this article is available at https://publons.com/publon/10.1111/ejn.15901.

DATA AVAILABILITY STATEMENT

Sample data and analysis code supporting the presented results are available on github (https://github.com/nivons/transitionnetworksNMDARE). With respect to the sensitivity of the data, de-identified data of the full sample will be provided upon reasonable request, subject to a material transfer agreement.

ORCID

Nina von Schwanenflug https://orcid.org/0000-0001-5573-259X
Juan P. Ramirez-Mahaluf https://orcid.org/0000-0002-0821-1174
Stephan Krohn https://orcid.org/0000-0003-0683-5386
Amy Romanello https://orcid.org/0000-0003-1257-9593
Josephine Heine https://orcid.org/0000-0001-5226-6650
Harald Prüss https://orcid.org/0000-0002-8283-7976
Nicolas A. Crossley https://orcid.org/0000-0002-3060-656X
Carsten Finke https://orcid.org/0000-0002-7665-1171

REFERENCES

Achard, S. (2006). A resilient, low-frequency, small-world human brain functional network with highly connected association cortical hubs. *Journal of Neuroscience*, *26*(1), 63–72. https://doi.org/10.1523/JNEUROSCI.3874-05.2006

Aerts, H., Fias, W., Caeyenberghs, K., & Marinazzo, D. (2016). Brain networks under attack: Robustness properties and the impact of lesions. *Brain*, *139*(12), 3063–3083. https://doi.org/10.1093/brain/aww194

Allen, E. A., Damaraju, E., Plis, S. M., Erhardt, E. B., Eichele, T., & Calhoun, V. D. (2014). Tracking whole-brain connectivity dynamics in the resting state. *Cerebral Cortex (New York, N.Y.: 1991)*, *24*(3), 663–676. https://doi.org/10.1093/cercor/bhs352

Bassett, D. S., Wymbs, N. F., Porter, M. A., Mucha, P. J., Carlson, J. M., & Grafton, S. T. (2011). Dynamic reconfiguration of human brain networks during learning. *Proceedings of*

14609568, 2023, 3, Downloaded from https://onlinelibrary.wiley.com/doi/10.1111/ejn.15901 by Charité - Universitaetsmedizin, Wiley Online Library on [24/03/2025]. See the Terms and Conditions (https://onlinelibrary.wiley.com/terms-and-conditions) on Wiley Online Library for rules of use; OA articles are governed by the applicable Creative Commons License

the National Academy of Sciences, *108*(18), 7641–7646. https://doi.org/10.1073/pnas.1018985108

Benjamini, Y., & Hochberg, Y. (1995). Controlling the false discovery rate: A practical and powerful approach to multiple testing. *Journal of the Royal Statistical Society: Series B (Methodological)*, *57*(1), 289–300. https://doi.org/10.1111/j.2517-6161.1995.tb02031.x

Bertolero, M. A., Yeo, B. T. T., & D'Esposito, M. (2015). The modular and integrative functional architecture of the human brain. *Proceedings of the National Academy of Sciences*, *112*(49), E6798–E6807. https://doi.org/10.1073/pnas.1510619112

Biswal, B., Zerrin Yetkin, F., Haughton, V. M., & Hyde, J. S. (1995). Functional connectivity in the motor cortex of resting human brain using echo-planar mri. *Magnetic Resonance in Medicine*, *34*(4), 537–541. https://doi.org/10.1002/mrm.1910340409

Cai, L., Liang, Y., Huang, H., Zhou, X., & Zheng, J. (2020). Cerebral functional activity and connectivity changes in anti-N-methyl-D-aspartate receptor encephalitis: A resting-state fMRI study. *NeuroImage: Clinical*, *25*, 102189. https://doi.org/10.1016/j.nicl.2020.102189

Calhoun, V. D., Miller, R., Pearlson, G., & Adalı, T. (2014). The Chronnectome: Time-varying connectivity networks as the next frontier in fMRI data discovery. *Neuron*, *84*(2), 262–274. https://doi.org/10.1016/j.neuron.2014.10.015

Chang, C., & Glover, G. H. (2010). Time–frequency dynamics of resting-state brain connectivity measured with fMRI. *NeuroImage*, *50*(1), 81–98. https://doi.org/10.1016/j.neuroimage.2009.12.011

Chen, Z., Zhou, J., Wu, D., Ji, C., Luo, B., & Wang, K. (2022). Altered executive control network connectivity in anti-NMDA receptor encephalitis. *Annals of Clinical and Translational Neurology*, *9*(1), 30–40. https://doi.org/10.1002/acn3.51487

Crossley, N. A., Mechelli, A., Vertes, P. E., Winton-Brown, T. T., Patel, A. X., Ginestet, C. E., McGuire, P., & Bullmore, E. T. (2013). Cognitive relevance of the community structure of the human brain functional coactivation network. *Proceedings of the National Academy of Sciences*, *110*(28), 11583–11588. https://doi.org/10.1073/pnas.1220826110

Dalmau, J., Armangué, T., Planagumà, J., Radosevic, M., Mannara, F., Leypoldt, F., Geis, C., Lancaster, E., Titulaer, M. J., Rosenfeld, M. R., & Graus, F. (2019). An update on anti-NMDA receptor encephalitis for neurologists and psychiatrists: Mechanisms and models. *The Lancet Neurology*, *18*(11), 1045–1057. https://doi.org/10.1016/S1474-4422(19)30244-3

Dalmau, J., Lancaster, E., Martinez-Hernandez, E., Rosenfeld, M. R., & Balice-Gordon, R. (2011). Clinical experience and laboratory investigations in patients with anti-NMDAR encephalitis. *The Lancet Neurology*, *10*(1), 63–74. https://doi.org/10.1016/S1474-4422(10)70253-2

de Vico Fallani, F., Aparecido, R. F., da Fontoura, C. L., Mattia, D., Cincotti, F., Astolfi, L., Vecchiato, G., Tabarrini, A., Salinari, S., & Babiloni, F. (2009). Analysis of the connection redundancy in functional networks from high-resolution EEG: A preliminary study. *Annual International Conference of the IEEE Engineering in Medicine and Biology Society*, *2009*, 2204–2207. https://doi.org/10.1109/IEMBS.2009.5334882

Deco, G., Jirsa, V. K., & McIntosh, A. R. (2011). Emerging concepts for the dynamical organization of resting-state activity in the brain. *Nature Reviews Neuroscience*, *12*(1), 43–56. https://doi.org/10.1038/nrn2961

Deco, G., Kringelbach, M. L., Jirsa, V. K., & Ritter, P. (2017). The dynamics of resting fluctuations in the brain: Metastability and its dynamical cortical core. *Scientific Reports*, *7*(1), 3095. https://doi.org/10.1038/s41598-017-03073-5

Eijlers, A. J. C., Wink, A. M., Meijer, K. A., Douw, L., Geurts, J. J. G., & Schoonheim, M. M. (2019). Reduced network dynamics on functional MRI signals cognitive impairment in multiple sclerosis. *Radiology*, *292*(2), 449–457. https://doi.org/10.1148/radiol.2019182623

Finke, C., Kopp, U. A., Prüss, H., Dalmau, J., Wandinger, K.-P., & Ploner, C. J. (2012). Cognitive deficits following anti-NMDA receptor encephalitis. *Journal of Neurology, Neurosurgery & Psychiatry*, *83*(2), 195–198. https://doi.org/10.1136/jnnp-2011-300411

Finke, C., Kopp, U. A., Scheel, M., Pech, L.-M., Soemmer, C., Schlichting, J., Leypoldt, F., Brandt, A. U., Wuerfel, J., Probst, C., Ploner, C. J., Prüss, H., & Paul, F. (2013). Functional and structural brain changes in anti-N-methyl-D-aspartate receptor encephalitis. *Annals of Neurology*, *74*(2), 284–296. https://doi.org/10.1002/ana.23932

Gibson, L. L., McKeever, A., Coutinho, E., Finke, C., & Pollak, T. A. (2020). Cognitive impact of neuronal antibodies: Encephalitis and beyond. *Translational Psychiatry*, *10*(1), 304. https://doi.org/10.1038/s41398-020-00989-x

Gibson, L. L., Pollak, T. A., Blackman, G., Thornton, M., Moran, N., & David, A. S. (2019). The psychiatric phenotype of anti-NMDA receptor encephalitis. *The Journal of Neuropsychiatry and Clinical Neurosciences*, *31*(1), 70–79. https://doi.org/10.1176/appi.neuropsych.17120343

Graus, F., Titulaer, M. J., Balu, R., Benseler, S., Bien, C. G., Cellucci, T., Cortese, I., Dale, R. C., Gelfand, J. M., Geschwind, M., Glaser, C. A., Honnorat, J., Höftberger, R., Iizuka, T., Irani, S. R., Lancaster, E., Leypoldt, F., Prüss, H., Rae-Grant, A., … Dalmau, J. (2016). A clinical approach to diagnosis of autoimmune encephalitis. *The Lancet. Neurology*, *15*(4), 391–404. https://doi.org/10.1016/S1474-4422(15)00401-9

Gu, S., Betzel, R. F., Mattar, M. G., Cieslak, M., Delio, P. R., Grafton, S. T., Pasqualetti, F., & Bassett, D. S. (2017). Optimal trajectories of brain state transitions. *NeuroImage*, *148*, 305–317. https://doi.org/10.1016/j.neuroimage.2017.01.003

Heine, J., Kopp, U. A., Klag, J., Ploner, C. J., Prüss, H., & Finke, C. (2021). Long-term cognitive outcome in anti–N-methyl-D-aspartate receptor encephalitis. *Annals of Neurology*, *90*(6), 949–961. https://doi.org/10.1002/ana.26241

Heine, J., Prüss, H., Bartsch, T., Ploner, C. J., Paul, F., & Finke, C. (2015). Imaging of autoimmune encephalitis—Relevance for clinical practice and hippocampal function. *Neuroscience*, *309*, 68–83. https://doi.org/10.1016/j.neuroscience.2015.05.037

Kringelbach, M. L., & Deco, G. (2020). Brain states and transitions: Insights from computational neuroscience. *Cell Reports*, *32*(10), 108128. https://doi.org/10.1016/j.celrep.2020.108128

Krohn, S., von Schwanenflug, N., Waschke, L., Romanello, A., Gell, M., Garrett, D. D., & Finke, C. (2021). A spatiotemporal complexity architecture of human brain activity [preprint]. *bioRxiv*. https://doi.org/10.1101/2021.06.04.446948

14609568, 2023, 3, Downloaded from https://onlinelibrary.wiley.com/doi/10.1111/ejn.15901 by Charité - Universitaetsmedizin, Wiley Online Library on [24/03/2025]. See the Terms and Conditions (https://onlinelibrary.wiley.com/terms-and-conditions) on Wiley Online Library for rules of use; OA articles are governed by the applicable Creative Commons License

Latora, V., & Marchiori, M. (2001). Efficient behavior of small-world networks. *Physical Review Letters*, *87*(19), 198701. https://doi.org/10.1103/PhysRevLett.87.198701

Loh, M., Rolls, E. T., & Deco, G. (2007). A dynamical systems hypothesis of schizophrenia. *PLoS Computational Biology*, *3*(11), e228. https://doi.org/10.1371/journal.pcbi.0030228

Lord, L.-D., Expert, P., Atasoy, S., Roseman, L., Rapuano, K., Lambiotte, R., Nutt, D. J., Deco, G., Carhart-Harris, R. L., Kringelbach, M. L., & Cabral, J. (2019). Dynamical exploration of the repertoire of brain networks at rest is modulated by psilocybin. *NeuroImage*, *199*, 127–142. https://doi.org/10.1016/j.neuroimage.2019.05.060

Lord, L.-D., Expert, P., Huckins, J. F., & Turkheimer, F. E. (2013). Cerebral energy metabolism and the brain's functional network architecture: An integrative review. *Journal of Cerebral Blood Flow & Metabolism*, *33*(9), 1347–1354. https://doi.org/10.1038/jcbfm.2013.94

Lynall, M.-E., Bassett, D. S., Kerwin, R., McKenna, P. J., Kitzbichler, M., Muller, U., & Bullmore, E. (2010). Functional connectivity and brain networks in schizophrenia. *Journal of Neuroscience*, *30*(28), 9477–9487. https://doi.org/10.1523/JNEUROSCI.0333-10.2010

Parkes, L., Fulcher, B., Yücel, M., & Fornito, A. (2018). An evaluation of the efficacy, reliability, and sensitivity of motion correction strategies for resting-state functional MRI. *NeuroImage*, *171*, 415–436. https://doi.org/10.1016/j.neuroimage.2017.12.073

Peer, M., Prüss, H., Ben-Dayan, I., Paul, F., Arzy, S., & Finke, C. (2017). Functional connectivity of large-scale brain networks in patients with anti-NMDA receptor encephalitis: An observational study. *The Lancet. Psychiatry*, *4*(10), 768–774. https://doi.org/10.1016/S2215-0366(17)30330-9

Power, J. D., Mitra, A., Laumann, T. O., Snyder, A. Z., Schlaggar, B. L., & Petersen, S. E. (2014). Methods to detect, characterize, and remove motion artifact in resting state fMRI. *NeuroImage*, *84*, 320–341. https://doi.org/10.1016/j.neuroimage.2013.08.048

Pruim, R. H. R., Mennes, M., van Rooij, D., Llera, A., Buitelaar, J. K., & Beckmann, C. F. (2015). ICA-AROMA: A robust ICA-based strategy for removing motion artifacts from fMRI data. *NeuroImage*, *112*, 267–277. https://doi.org/10.1016/j.neuroimage.2015.02.064

Ramirez-Mahaluf, J. P., Medel, V., Tepper, Á., Alliende, L. M., Sato, J. R., Ossandon, T., & Crossley, N. A. (2020). Transitions between human functional brain networks reveal complex, cost-efficient and behaviorally-relevant temporal paths. *NeuroImage*, *219*, 117027. https://doi.org/10.1016/j.neuroimage.2020.117027

Rolls, E. T. (2012). Glutamate, obsessive–compulsive disorder, schizophrenia, and the stability of cortical attractor neuronal networks. *Pharmacology Biochemistry and Behavior*, *100*(4), 736–751. https://doi.org/10.1016/j.pbb.2011.06.017

Rolls, E. T. (2021). Attractor cortical neurodynamics, schizophrenia, and depression. *Translational Psychiatry*, *11*(1), 215. https://doi.org/10.1038/s41398-021-01333-7

Shine, J. M., Koyejo, O., Bell, P. T., Gorgolewski, K. J., Gilat, M., & Poldrack, R. A. (2015). Estimation of dynamic functional connectivity using multiplication of temporal derivatives. *NeuroImage*, *122*, 399–407. https://doi.org/10.1016/j.neuroimage.2015.07.064

Sporns, O., & Betzel, R. F. (2016). Modular brain networks. *Annual Review of Psychology*, *67*(1), 613–640. https://doi.org/10.1146/annurev-psych-122414-033634

Tognoli, E., & Kelso, J. A. S. (2014). The metastable brain. *Neuron*, *81*(1), 35–48. https://doi.org/10.1016/j.neuron.2013.12.022

von Schwanenflug, N., Krohn, S., Heine, J., Paul, F., Prüss, H., & Finke, C. (2022). State-dependent signatures of anti-*N*-methyl-D-aspartate receptor encephalitis. *Brain Communications*, *4*(1), fcab298. https://doi.org/10.1093/braincomms/fcab298

Yeo, B. T., Krienen, F. M., Sepulcre, J., Sabuncu, M. R., Lashkari, D., Hollinshead, M., Roffman, J. L., Smoller, J. W., Zöllei, L., Polimeni, J. R., Fischl, B., Liu, H., & Buckner, R. L. (2011). The organization of the human cerebral cortex estimated by intrinsic functional connectivity. *Journal of Neurophysiology*, *106*(3), 1125–1165. https://doi.org/10.1152/jn.00338.2011

SUPPORTING INFORMATION

Additional supporting information can be found online in the Supporting Information section at the end of this article.

How to cite this article: von Schwanenflug, N., Ramirez-Mahaluf, J. P., Krohn, S., Romanello, A., Heine, J., Prüss, H., Crossley, N. A., & Finke, C. (2023). Reduced resilience of brain state transitions in anti-*N*-methyl-D-aspartate receptor encephalitis. *European Journal of Neuroscience*, *57*(3), 568–579. https://doi.org/10.1111/ejn.15901

14609568, 2023, 3, Downloaded from https://onlinelibrary.wiley.com/doi/10.1111/ejn.15901 by Charité - Universitaetsmedizin, Wiley Online Library on [24/03/2025]. See the Terms and Conditions (https://onlinelibrary.wiley.com/terms-and-conditions) on Wiley Online Library for rules of use; OA articles are governed by the applicable Creative Commons License